EFFECT OF ZnS ON QUANTUM DOT CHARACTERISTIC AND QUANTUM DOT LIGHT-EMITTING DIODE PERFORMANCE

MINH-SON HOANG[1*], NHAT-TRUONG LO[1], VIET-HUNG THAI[1,] and HSUEH-SHIH CHEN[2]
[1] *Faculty of Chemical Engineering, Industrial University of Ho Chi Minh University, Ho Chi Minh City, Vietnam*
[2] *Department of Materials Science and Engineering, National Tsing Hua University, Hsinchu, Taiwan*
**Corresponding author: hoangminhson@iuh.edu.vn*
DOIs: https://www.doi.org/10.46242/jstiuh.v80i2.5900

Abstract. The structural configuration of quantum dots plays a crucial role in determining their optical properties and performance in specific applications. Encapsulating the quantum dot core with a ZnS shell to form a core/shell architecture enhances the photoluminescence emission spectrum, yielding a narrower full width at half maximum (FWHM) and thereby indicating superior color purity. Moreover, quantum dot light-emitting diodes (QDLEDs) incorporating core/shell quantum dots demonstrate improved performance in terms of luminance, current efficiency, and device lifetime stability. This enhanced efficiency is primarily attributed to the ZnS shell, which effectively reduces surface defects and facilitates carrier injections, highlighting the strong potential of core/shell quantum dots for advanced optoelectronic devices.
Keywords. Quantum dot, quantum dot light-emitting diodes.

1 INTRODUCTION

Quantum dots (QDs), classified as advanced zero-dimensional semiconductor materials, have attracted extensive research over the past three decades due to their exceptional optical properties.[1] These include size-dependent emission tunability, narrow spectral bandwidth, and high quantum yield (QY). The luminescent characteristic of QDs is highly dependent on their structural configuration.[2] Common structural types include core/shell, gradient alloy, and homogeneous alloy architectures, each synthesized to enhance optical and electronic performance.[3] Common structural type as only core quantum dots has been applied in various devices, however, their performance may rapidly degrade due to the inherently low quality of QDs.[4] For instance, core/shell structure in which the shell plays a critical role in determining both luminescence efficiency and electrical characteristic relative to quantum dot optoelectronic devices. Furthermore, the choice of shell materials typically affects the QD optical properties. Materials such as CdS, HgS or ZnS, have been widely used to protect QD core, thereby enhancing overall quality.[5] However, due to toxicity of heavy elements like Cd and Hg, their utilization is increasingly restricted in certain applications,[6] therefore, ZnS has emerged as a more favorable for shell composition.

Given the diversity in structural design and emission properties, QDs hold significant promises for several applications in photoluminescent and electroluminescent devices, including QDLEDs, and other optoelectronic devices such as photo-voltaic, photodiode.[7] Particularly, QDLEDs are considered strong candidate for next-generation display based on their advantages such as high color purity, high quantum efficiency, all-solution processability, and cost-effective fabrication suitable for large-area display and flexible devices.[8]

In this study, the electrical performance of QDLED incorporating two distinct QD structures was evaluated to determine the effect of QD structure on device efficiency. The ZnS shield around QD core was found to balance the carrier injection and suppress the Auger recombination, thereby enhancing device performance. Therefore, QDLED utilizing the core/shell QDs achieved the better performance with a maximum brightness and current efficiency of 168300 $cd \cdot m^{-2}$ and 20.47 $cd \cdot A^{-1}$, respectively, highlighting their potential for integration into optoelectronic devices.

2 EXPERIMENT

Two types of green QDs were supplied by Hsinlight Inc (Taiwan): QD1, consisting solely of an alloyed core, and QD2, comprising an alloyed core encapsulated by a ZnS shell, as shown in Figure 1a. As-received QDs were dispersed in toluene and subsequently purified through a multi-step process. Initially, methanol

was employed to precipitate QDs via centrifugation, followed by redispersion in octane at a concentration of 30 mg·mL^{-1} for further device preparation.

QDLED device architecture considered of the following layers: ITO/Pedot:PSS/PVK/QD/ZnO/Al, functioning respectively as the anode, hole injection layer (HIL), hole transport layer (HTL), emissive layer (EML), electron transport layer (ETL), and cathode. Indium tin oxide (ITO) substrates were subsequently cleaned using deionized water, acetone, isopropyl alcohol, and UV-ozone. Pedot:PSS (referred to as Pedot for short) was spin-coated onto the substrate and baked at 150ºC to form HIL. Subsequently, the HTL was deposited by spin-coating a PVK solution onto the Pedot layer, followed by thermal treatment at 150ºC. The QDs solution was then spin-coated at 3000 rpm to form the EML. ZnO was deposited via spin-coating and heated at 60ºC. Finally, Al cathode was thermally evaporated under high vacuum, and device encapsulation was carried in N_2-filled glovebox. QDLED incorporating QD1 was denoted as QD1-LED, while device using QD2 was designated as QD2-LED.

Photoluminescence (PL) and Electroluminescence (EL) spectra were recorded using Edinburgh FS5 spectrofluorometer. The UV-absorption was obtained with a Jasco V-770 spectrophotometer. The QD materials were characterized using transmission electron microscope (TEM) JEOL JEM-F200.

Current-voltage (I-V) characteristics of both QDLED and single carrier devices were measured with Keithley 2450 source meter. The luminance of devices evaluated with luminance meter (Topcon BM-9A). The turn-on voltage of QDLED was defined as the value at which the device brightness reached 1 cd·m^{-2}.

3 RESULT AND DISCUSSION

3.1 Quantum dot optical properties

The structural configuration of QDs plays a vital role in determining their optical characteristics as well as the performance of optoelectronic applications. Figure 1a presents the illustrated graphic of QD, QD1 consists solely of an alloyed core, whereas QD2 comprises an alloyed core encapsulated by a ZnS shell. QD1 exhibits photoluminescence (PL) emission spectra with a peak wavelength of 532 nm and a FWHM of 33 nm. In contrast, QD2 demonstrates a blue-shifted peak at 523 nm with a narrower FWHM of 17 nm, respectively. This spectral shift is attributed to the core etching process during the QDs synthesis,[9] which reduce the core size prior to ZnS growth. The ZnS shell effectively passivate the alloy core, reducing the surface defects and thereby enhancing the overall quality of the QDs.[10] In addition, the reduced FWHM observed in QD2 indicates a lower defect density and more uniform particle size distribution compared to QD1.[11] Transmission electron microscopy (TEM) images in Figure 1b-c reveal that QD1 has average diameter of ~5.5 nm, slightly smaller than 8.8 nm observed for QD2, indicating that the shell growth contributes to an increase in particles size.

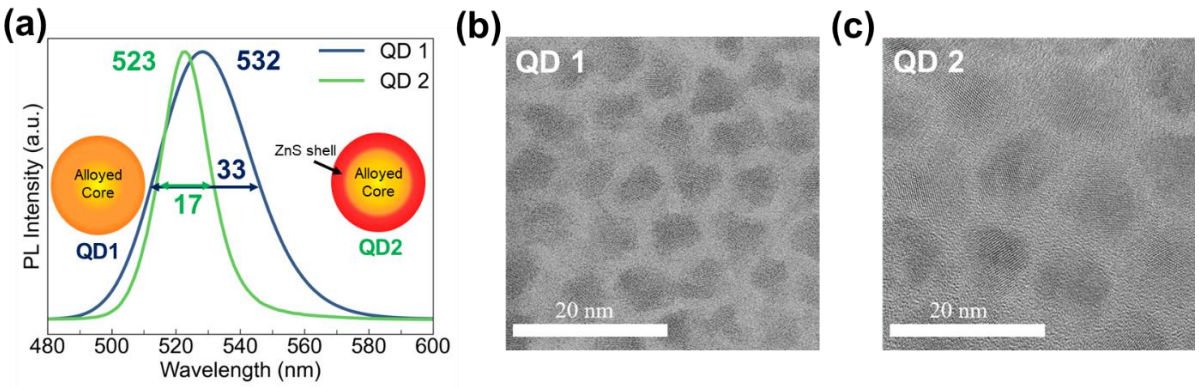

Figure 1. Structural representations of two types of quantum dots alongside their PL spectra: (a) QD1 featuring an alloyed core, and QD2 comprising an alloyed core with a ZnS shell. (b, c) TEM images corresponding to QD1 and QD2, the scale bar is 20 nm.

3.2 QDLED performance

QDLEDs were fabricated with the same structure of Pedot/PVK/QDs/ZnO/Al (as shown in Figure 2a) Two distinct QD types, QD1 and QD2, were employed and the resulting devices are denoted as QD1-LED and QD2-LED, respectively. All fabrication steps were conducted under ambient conditions, except for the deposition of Al cathode, which was carried out via thermal evaporator under high vacuum.

Figure 2b presents the comparison of device performance for QD1- and QD2-LEDs. QD1-LED exhibits a lower turn-on voltage of 2.6 V, compared to 5 V for the QD2-based device. However, QD2-LED demonstrates superior performance, achieving a maximal luminance of 168300 $cd{\cdot}m^{-2}$ and a peak current efficiency of 20.47 $cd{\cdot}A^{-1}$, significantly outpacing 39000 $cd{\cdot}m^{-2}$ and 8.91 $cd{\cdot}A^{-1}$ recorded of QD1-LED. The relatively lower turn-on voltage of QD1-LED might be attributed to the alloyed structure of its QDs, which can facilitate more carrier injections thereby enhancing current densities for device working at low voltage (dark-blue curve in Figure 2b). In contrast, QD2 features a ZnS shell that introduces an energy barrier due to its high conduction band and low valence band levels, promoting carrier confinement within the emissive layer.[12] This energy barrier necessitates high operating voltage to overcome carrier injection resistance, but it assistingly balance carriers injection into the QD core, suppresses current leakage, and enhances recombination efficiency, thereby improving device performance.[13-15] The structural differences between QD1 and QD2 are further reflected in their voltage-dependent efficiency behavior. It is noted that QD1-LED exhibits high current density with rising voltage, but its brightness remains limited, indicating inefficiency and resulting in efficiency roll-off. Conversely, QD2-LED achieves lower current density at higher voltages while achieving better brightness, and sustained efficiency, signifying greater operational stability under high electric fields (Figure 2c). A summary of device performance is listed in Table 1.

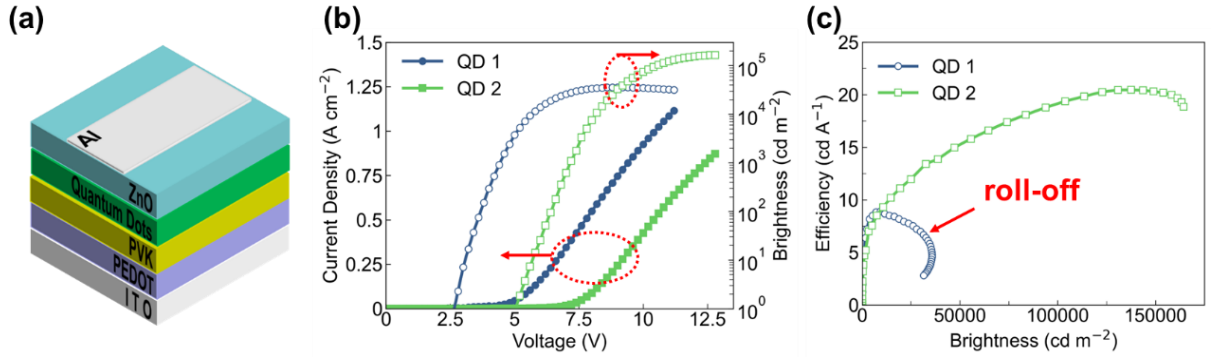

Figure 2. (a) Schematic of the QDLED device structure. Comparison of QDLED performance using two distinct quantum dot structures, QD1 and QD2. (b) Current density and brightness as a function of applied voltage. (c) Current efficiency as a function of brightness.

Table 1. Summarized device performance of QDLEDs with different QD structure

Device	QDs structure	Turn-on voltage (V)	Max. Brightness ($cd{\cdot}m^{-2}$)	Max. CE ($cd{\cdot}A^{-1}$)	Max EQE (%)
QD1	Alloy core	2.6	39000	8.91	2.54
QD2	Alloy core/ZnS shell	5	168300	20.47	5.82

To further examine the carrier injection characteristics of different QDs, hole-only and electron-only devices were fabricated with the following structure: ITO/Pedot/PVK/QDs/MoO_3/Al and ITO/ZnO/QDs/ZnO/Al, respectively. Figure 3a illustrates the significant deviation between the hole and electron injection curves for QD1, indicating an obvious imbalance in carrier injection. This difference leads to excess electron accumulation within the QDs, resulting in exciton injection quenching via Auger recombination process,[16, 17] which negatively affects the performance of QD1-LED. In contrast, the

electron and hole injection curves for QD2 exhibit close alignment, suggesting a more balanced carrier distribution within EML (Figure 3b). This balance contributes to the superior efficiency observed in QD2-LED compared to QD1-LED. The improved performance is ascribed to the presence of a ZnS shell in QD2, which acts as an energy barrier that moderates electron injections, thereby matching it with hole injections and enhancing carrier confinement.

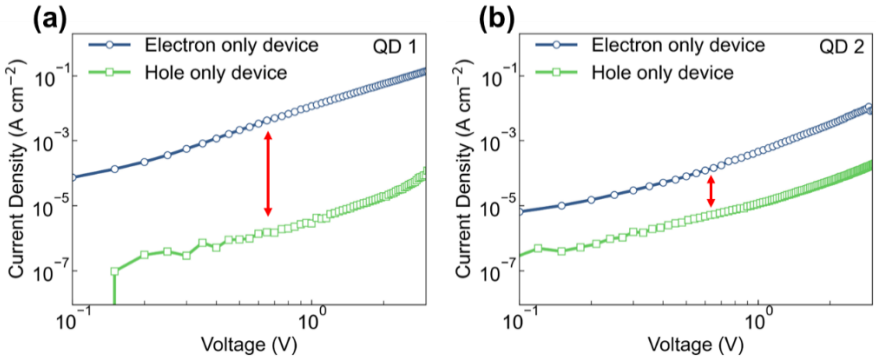

Figure 3. Comparison of single-carrier devices with different quantum dot structures: (a) QD1 and (b) QD2.

The operation stability of QDLED was additionally assessed by measuring device lifetimes under current of 10 mA, as shown in Figure 4a. Device incorporating QD2 exhibit significantly longer lifetimes and high performance compared to those using QD1. These results clearly indicate that QD2 offers enhanced stability during device operation. Furthermore, infrared (IR) thermal imaging reveals that the operating temperature of QD1-LED under the same constant current is consistently higher than that of QD2-LED (Figure 4b-c). This inflated temperature may be attributed to Auger recombination, which is caused by the severe carrier injection imbalance. Such thermal effects can accelerate device degradation and reduce overall lifetime.[18]

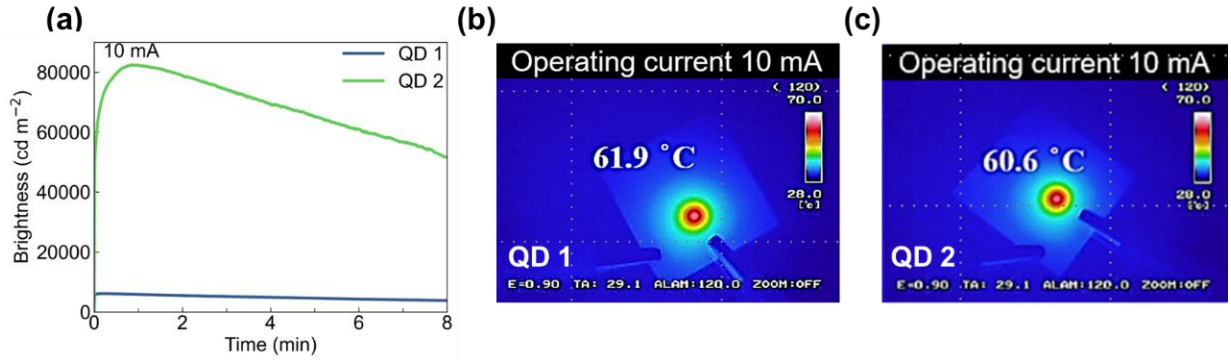

Figure 4. (a) Operational lifetime of QDLEDs under a constant current of 10 mA. Infrared thermal images of devices incorporating (b) QD1 and (c) QD2.

In addition, the optical characteristics of QDLED were evaluated through EL spectra measured under varying driving voltages as shown in Figure 5. QD1-based devices exhibit a redshift of ~5 nm their EL peak positions (from 534 to 539 nm), whereas QD2-based devices show a shift of ~3 nm within a range of 523 to 526 nm, as the applied voltage increasing from 6 to 12 V. The FWHM of EL peaks broaden by 3.63 nm for QD1, which is greater than the 0.59 nm widening observed for QD2. The EL spectra wide broadening in QD1 may be related to its electrical characteristic, particularly the imbalance in carrier injection that promotes the Auger recombination and heat generation.[19] Excess electrons are likely to interact with phonons, resulting in energy loss subsequent recombination with holes at uncertain energy level, thereby contributing to the broadening of EL spectrum. The observed redshift in both devices may also be impacted by the quantum-confined Stark effect.[20] The imbalance in carrier injection leads to enhanced Auger recombination and thermal effects, which in turn cause energy dissipation through electron-phonon interactions.[21] From optical perspective, both QDs exhibit EL peak redshift, but QD1

suffers from significant spectral broadening. It presents a critical limitation for display applications, as it affects the color purity and further reduces display resolution. Based on these findings, QD2-with its core/shell structure-appears as a favored candidate for integration into optoelectronic devices.

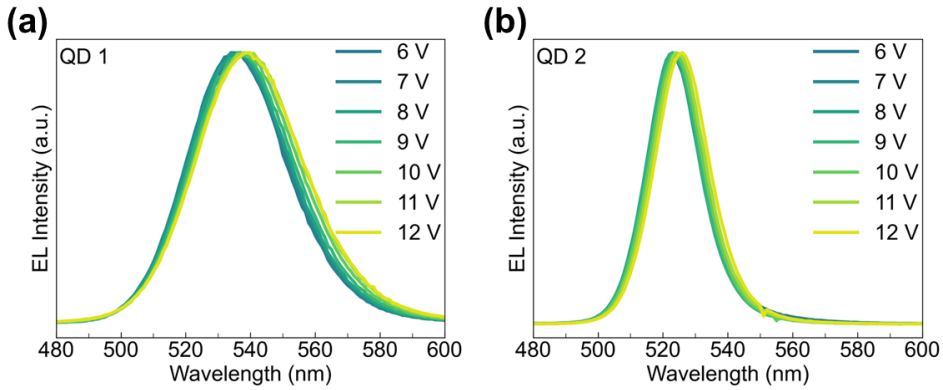

Figure 5. Electroluminescence (EL) spectra of QDLEDs with (a) QD1 and (b) QD2, measured under driving voltages ranging from 6 V to 12 V.

4 CONCLUSION

The effect of QD structure was clearly demonstrated through the optical characterization. Core/shell QD2 obtained a slightly larger particle size and a narrower PL peak compared to QD1, improving the spectra purity. Additionally, QDLED incorporating QD2 showed enhanced device performance. The ZnS shell in QD2 contributes to more balance carrier injections, resulting in higher luminance and current efficiency relative to QD1-based devices. This finding emphasizes the critical role of QD structural design in optimizing the performance of optoelectronic devices to achieve stable operation and maximize device efficiency.

ACKNOWLEDGMENT

The authors would like to thank QLab (Department of Materials Science and Engineering, National Tsing Hua University, Taiwan) and the company Hsinlight Inc., Taiwan for providing the facilities and materials necessary for this study. The authors would like to express their gratitude to Syskey Technology Co. Ltd., Taiwan for the kind support of the evaporation system.

REFERENCES

[1] N. Tessler, V. Medvedev, M. Kazes, S. Kan, and U. Banin, "Efficient near-infrared polymer nanocrystal light-emitting diodes," (in eng), *Science*, vol. 295, no. 5559, pp. 1506-8, 2002.

[2] M. D. Regulacio and M.-Y. Han, "Composition-Tunable Alloyed Semiconductor Nanocrystals," *Acc. Chem. Res.*, vol. 43, no. 5, pp. 621-630, 2010.

[3] K. Ba and J. Wang, "Advances in solution-processed quantum dots based hybrid structures for infrared photodetector," *Mater. Today*, vol. 58, pp. 119-134, 2022.

[4] A. Sahu and D. Kumar, "Core-shell quantum dots: A review on classification, materials, application, and theoretical modeling," *J. Alloys Compd.*, vol. 924, p. 166508, 2022.

[5] A. R. AbouElhamd, K. A. Al-Sallal, and A. Hassan, "Review of Core/Shell Quantum Dots Technology Integrated into Building's Glazing," *Energies*, vol. 12, no. 6, p. 1058.

[6] Y. Sung, J. Chang, S. Choi, and S. Jeong, "Synthesis Strategies and Applications of Non-toxic Quantum Dots," *Korean J. Chem. Eng.*, vol. 41, no. 13, pp. 3317-3343, 2024.

[7] J. Lee, V. C. Sundar, J. R. Heine, M. G. Bawendi, and K. F. Jensen, "Full Color Emission from II–VI Semiconductor Quantum Dot–Polymer Composites," *Adv. Mater.*, vol. 12, no. 15, pp. 1102-1105, 2000.

[8] Y. Sun, Y. Jiang, X. W. Sun, S. Zhang, and S. Chen, "Beyond OLED: Efficient Quantum Dot Light-Emitting Diodes for Display and Lighting Application," *Chem. Rec.*, vol. 19, no. 8, pp. 1729-1752, 2019.

[9] S. A. Al Muyeed, X. Wei, D. Borovac, R. Song, N. Tansu, and J. J. Wierer, "Controlled growth of InGaN quantum dots on photoelectrochemically etched InGaN quantum dot templates," *J. Cryst. Growth*, vol. 540, p. 125652, 2020.
[10] S. Yin *et al.*, "Enhanced Surface Passivation of Lead Sulfide Quantum Dots for Short-Wavelength Photodetectors," *Chem. Mater.*, vol. 34, no. 12, pp. 5433-5442, 2022.
[11] C. Zhou *et al.*, "Comparative study of photoluminescence for type-I InAs/GaAs0.89Sb0.11 and type-II InAs/GaAs0.85Sb0.15 quantum dots," *Opt. Mater.*, vol. 98, p. 109479, 2019.
[12] M. Hbibi *et al.*, "Finite confinement potentials, core and shell size effects on excitonic and electron-atom properties in cylindrical core/shell/shell quantum dots," *Sci. Rep.*, vol. 12, no. 1, p. 14854, 2022.
[13] W. Ji, P. Jing, W. Xu, X. Yuan, Y. Wang, J. Zhao, and A. K.-Y. Jen, "High color purity ZnSe/ZnS core/shell quantum dot based blue light emitting diodes with an inverted device structure," *Appl. Phys. Lett.*, vol. 103, no. 5, 2013.
[14] Y.-H. Kim *et al.*, "Efficient, operation-stable green ZnSeTe quantum dot-light-emitting diodes: Impacts of shell dimension and Al incorporation," *Chem. Eng. J.*, vol. 522, p. 167742, 2025.
[15] H. Zhang *et al.*, "High-Efficiency Green InP Quantum Dot-Based Electroluminescent Device Comprising Thick-Shell Quantum Dots," *Adv. Opt. Mater.*, vol. 7, no. 7, p. 1801602, 2019.
[16] F. Wang *et al.*, "Achieving Balanced Charge Injection of Blue Quantum Dot Light-Emitting Diodes through Transport Layer Doping Strategies," *J. Phys. Chem. Lett.*, vol. 10, no. 5, pp. 960-965, 2019.
[17] H. Qi, S. Wang, X. Jiang, Y. Fang, A. Wang, H. Shen, and Z. Du, "Research progress and challenges of blue light-emitting diodes based on II–VI semiconductor quantum dots," *J. Mater. Chem. C*, vol. 8, no. 30, pp. 10160-10173, 2020.
[18] S. Mokarian Zanjani, S. Sadeghi, A. Shahalizad, and M. Pahlevani, "An investigation on the cyclic temperature-dependent performance behaviors of ultrabright air-stable QLEDs," *Sci. Rep.*, vol. 13, no. 1, p. 12713, 2023.
[19] J. A. Brum and G. Bastard, "Electric-field-induced dissociation of excitons in semiconductor quantum wells," *Phys. Rev. B*, vol. 31, no. 6, pp. 3893-3898, 1985.
[20] J. W. Christopher, B. B. Goldberg, and A. K. Swan, "Long tailed trions in monolayer MoS2: Temperature dependent asymmetry and resulting red-shift of trion photoluminescence spectra," *Sci. Rep.*, vol. 7, no. 1, p. 14062, 2017.
[21] W. Xiang *et al.*, "Ba-induced phase segregation and band gap reduction in mixed-halide inorganic perovskite solar cells," *Nat. Commun.*, vol. 10, no. 1, p. 4686, 2019.

ẢNH HƯỞNG CỦA LỚP VỎ ZnS ĐẾN ĐẶC TÍNH CỦA CHẤM LƯỢNG TỬ VÀ HIỆU SUẤT CỦA ĐI-ỐT PHÁT QUANG CHẤM LƯỢNG TỬ

HOÀNG MINH SƠN*[1], LỘ NHẬT TRƯỜNG[1], THÁI VIỆT HƯNG[1], CHEN HSUEH SHIH[2]

[1] Khoa Công nghệ Hóa học, Trường Đại học Công nghiệp TP.HCM, Việt Nam

[2] Khoa Khoa học và Kỹ thuật Vật liệu, ĐH Quốc gia Thanh Hoa, Đài Loan

** Tác giả liên hệ: hoangminhson@iuh.edu.vn*

Tóm tắt. Cấu trúc của chấm lượng tử đóng vai trò quan trọng trong việc quyết định các đặc tính quang học và hiệu suất của chúng trong từng ứng dụng cụ thể. Việc bao bọc lõi chấm lượng tử bằng lớp vỏ ZnS để tạo thành cấu trúc lõi/vỏ giúp cải thiện phổ phát quang, làm cho độ rộng phổ tại nửa cực đại (FWHM) hẹp hơn, từ đó thể hiện độ tinh khiết màu sắc cao hơn. Ngoài ra, các đi-ốt phát quang chấm lượng tử (QDLEDs) sử dụng chấm lượng tử với cấu trúc lõi/vỏ cho thấy hiệu suất vượt trội về độ sáng, hiệu suất dòng điện và độ ổn định tuổi thọ thiết bị. Hiệu suất được cải thiện này chủ yếu nhờ vào lớp vỏ ZnS, vốn có khả năng giảm khuyết tật bề mặt và hỗ trợ quá trình tiêm tải điện, cho thấy tiềm năng mạnh mẽ của chấm lượng tử lõi/vỏ trong các thiết bị quang điện tử tiên tiến.
Từ khóa. Chấm lượng tử, đi-ốt phát quang chấm lượng tử.

Received on October 04 – 2025

Revised on December 11 - 2025